From ab Initio Calculations to Model Hamiltonians: The Effective Hamiltonian Technique as an Efficient Tool to Describe Mixed-Valence Molecules

Hélène Bolvin*

Laboratoire de Chimie Quantique, Institut Le Bel, UMR 7551 CNRS/Université Louis Pasteur, 4 rue Blaise Pascal 67000 Strasbourg, France

Received: January 22, 2003; In Final Form: April 9, 2003

The excitation spectrum of the Creutz−Taube molecule in slightly modified form, that is, [HCN $(NH_3)_4$ Ru pz Ru $(NH_3)_4$ NCH]$^{5+}$, where pz = pyrazine, is calculated with wave function-based ab initio methods. An effective matrix is built using Bloch's procedure in a model space generated by the d orbitals of the ruthenium atoms and the lowest π^* orbital of the bridging ligand. A model Hamiltonian is deduced. The effect of the mixing of the orbitals is discussed. A large part of the spectrum (33 states) can be well described in terms of two parameters: *t*, the transfer integral between a d orbital of the ruthenium and the π^* orbital, and *U*, the excitation energy from the d orbital to the π^* orbital. These parameters have been estimated at different levels of correlation: the dynamical correlation mostly affects *U*, which is negative without correlation and becomes almost zero with correlation. This article shows that a two-band Hubbard Hamiltonian is an excellent model for describing bridged mixed-valence molecules and proposes a procedure that allows the determination of the parameters of this model Hamiltonian by wave function-based ab initio calculations.

1. Introduction

The synthesis of the so-called Creutz−Taube molecule[1] has been the starting point for the study of mixed-valence polynuclear compounds (i.e., compounds made of two or more redox sites existing in different oxidation states). Whether homonuclear or heteronuclear, they are good candidates for electron or energy transfer and can exhibit other interesting properties (e.g., in nonlinear optics and magnetism, they are prototypes of molecular electric wires in nanotechnology). A comprehensive review is given in ref 2. In the case of homonuclear binuclear species, the migrating electron can be trapped on one site, breaking the symmetry of the molecule, or it can be delocalized on two sites; the behavior is determined by the strength of an electronic parameter V_{AB} compared to the relaxation energy gained by the localization of the electron. V_{AB} is the electronic coupling between the two states with one electron localized on one site, and it describes the ability of the excess electron to transfer from one site to the other. V_{AB} is measured experimentally through the energy or intensity of the intervalence transition, namely, the optical transition that couples the two former states. For delocalized systems, the intervalence transition energy is a direct measure of the V_{AB} parameter whereas for localized or partially localized systems it is related to V_{AB} assuming that the potential curves are parabolas.[3] V_{AB} is one of the key parameters determining the system's behavior. It has been studied in terms of the nature and length of the bridging ligand;[4] because of the distance between the metallic centers, the coupling is not direct but occurs through the ligands, either through the virtual (electron transfer) or the occupied orbitals (hole transfer) of the bridging ligand.

Models have been proposed to describe this superexchange mechanism.[5] The system is formally divided into units: the two metallic units form the two end groups, and the chemical entities of the bridge form the intermediate units. One works in the tight-binding approximation, taking into account only the interactions between nearest neighbors. Different techniques based on the perturbation theory approximations to express V_{AB} in terms of the electronic parameters of the bridging ligand have been used: the Löwdin partitioning method,[6] time-independent[7] and time-dependent[8] propagator techniques, or a nonperturbative time-dependent procedure based on the effective Hamiltonian technique.[9] Let us consider the simple case of a bridge built from *m* identical units numbered from 2 to $m + 1$ and two identical metallic centers numbered 1 and $m + 2$. One considers a model Hamiltonian $\hat{H}_m$ built in the basis of the $\{|\chi_j\rangle\}_{j=1,m+2}$, where $|\chi_j\rangle$ is the wave function of the system with the excess electron localized on unit *j*. One denotes *t* the metal−ligand and t_{int} the intraligand coupling parameters: $t = \langle\chi_1|\hat{H}_m|\chi_2\rangle = \langle\chi_{m+1}|\hat{H}_m|\chi_{m+2}\rangle$, and $t_{int} = \langle\chi_j|\hat{H}_m|\chi_{j+1}\rangle$ ($j = 2, m$). Denoting *U* the excitation energy from states $|\chi_1\rangle$ or $|\chi_{m+2}\rangle$ to states $|\chi_{j+1}\rangle$ ($j = 1, m$), the effective coupling between the end groups can be expressed as

$$V_{AB} = 2\left(\frac{t^2}{-U}\right)\left(\frac{t_{int}}{-U}\right)^{m-1} \quad (1)$$

provided that $|t/U| \ll 1$, as was first demonstrated by McConnell.[10] Whatever the refinement of the model, they are all based on the representation of the molecule divided into subunits and the stipulation that states $|\chi_1\rangle$ and $|\chi_{m+2}\rangle$ are well separated in energy from the other ones.

This modeling of the bridged mixed-valence compounds is still in use: the competition between the superexchange and the charge-hopping or sequential mechanisms can be expressed in terms of *t* and *U*,[11,12] and the influence of the solvent effects on the bridge-mediated charge transfer can be discussed in terms of these parameters as well.[13] The vibronic analysis of these systems can be done in terms of a three-level system described by these parameters.[14] The properties of these compounds are well reproduced by modeling the electronic properties by a two-

* E-mail: helene.bolvin@quantix.u-strasbg.fr.

10.1021/jp034176+ CCC: $25.00
Published on Web 06/03/2003

band Hubbard Hamiltonian:[15]

$$\hat{H}_{\mathrm{el}} = \sum_{j,\sigma}^{N_{\mathrm{site}}} \epsilon_j n_{j,\sigma} + t \sum_{j,\sigma}^{N_{\mathrm{site}}-1} (a_{j,\sigma}^{+} a_{j+1,\sigma} + h.c.) + u \sum_{j(M\ \mathrm{only})} n_{j,\uparrow}\, n_{j,\downarrow} \tag{2}$$

as first introduced by Ondrechen et al.[16] In eq 2, ϵ_j is the site energy, u is the on-site repulsion, t is the $d - \pi^*$ resonance integral, and $a_{j\sigma}$ ($a_{j\sigma}^{+}$) is the annihilation (creation) operator for one electron in the orbital of site j with spin σ and $n_{j,\sigma} = a_{j\sigma}^{+} a_{j\sigma}$. Furthermore, Ferretti et al.[17] described the nuclear degrees of freedom by harmonic oscillators that couple by a linear vibronic coupling to the electronic properties. They first described mixed-valence chains and then modeled bridged dimers; they reproduce the essential features of the electroabsorption spectra.[18] With $\Delta = \epsilon_{\mathrm{L}} - \epsilon_{\mathrm{M}}$ (L and M denoting ligand and metal, respectively), the link with the previous model is obviously obtained with $U = \Delta - u$. The discussion in terms of the two parameters t and U is usually qualitative, but there have been some attempts to evaluate them from experiment. Zwickel et al.[19] deduced them by comparing the charge-transfer spectra of $(NH_3)_5Ru\ L^{2+}$ and *cis*- and *trans*-$(NH_3)_4Ru\ L_2^{2+}$, and they found for L = pyrazine that $t = 6600\ cm^{-1}$ and $U = 16\,700\ cm^{-1}$. Creutz et al.[20] have evaluated t by the Hush equation in the monomer taking $r_{ab} = 3.5$ Å and have deduced U from the energy of the MLCT band (metal-to-ligand charge transfer): they found $t = 5700\ cm^{-1}$ and $U = 17\,900\ cm^{-1}$. Ferretti et al.[21] found $t = 5900\ cm^{-1}$, $u = 37300\ cm^{-1}$, and $\Delta = 40\,800\ cm^{-1}$ by numerically fitting the experimental absorption bands of the $[(NH_3)_5Ru\text{-pz-}Ru(NH_3)_5]^{n+}$ systems with $n = 4$ and 5 with the previous Hubbard Hamiltonian. (It follows that $U = 3500\ cm^{-1}$.) The values of t are very similar, but the values of U are different because the two first values deal with a mononuclear molecule and the third one deals with a binuclear one. It is the goal of this study to provide more insight into the definition and the quantitative evaluation of these parameters, and we show that they can be calculated using the energies as well as the wave functions of the first excited states.

The effective Hamiltonian methodology gives a procedure to project information of some exact wave function onto a relevant reduced subspace.[22] It has already been used to describe the electron-transfer phenomenon as already mentioned though the Löwdin partitioning method[6] or the Bloch transformation:[9] in these cases, the transformation was used to concentrate the information from a model space including the orbitals of the bridging ligand (generated by the $\{|\chi_j\rangle\}_{j=1,m+2}$) onto a smaller model space restricted to the two orbitals of the metals ($|\chi_1\rangle$ and $|\chi_{m+2}\rangle$) to evaluate the superexchange contribution to the effective coupling V_{AB}, that is, to express V_{AB} in terms of local couplings, as was done in eq 1. In this paper, we use the effective Hamiltonian procedure upstream compared to the procedure used in the cited works: the idea is to build the model Hamiltonian including the orbitals of the bridging ligands from ab initio calculations of the whole molecule. Recently, the group of Malrieu has used this procedure to build the whole valence matrix in a space including the ionic configurations in some magnetic binuclear complexes[23] and was able to evaluate effective parameters such as t, the effective hopping parameter between the magnetic orbitals, and U, the energy gap between the covalent and ionic configurations. This technique had been used previously to evaluate the V_{AB} coupling either at the extended Hückel molecular orbital level,[24] in a second-order perturbation theory approach, or through a limited CI (configuration interaction).[25] In this work, it is applied to a bridged mixed-valence complex including the orbitals of the bridging ligand in the model space. The molecular system is divided into three units: two metallic atoms with three active d orbitals each and an organic aromatic bridge with an active π^* orbital. We focus on the methodology: how to derive the effective Hamiltonian from the ab initio calculations and how to deduce a model Hamiltonian from the effective one. We follow here the terminology proposed by Durand and Malrieu:[22] an effective Hamiltonian is obtained by the projection of some exact wave functions onto a finite model space, and a model Hamiltonian is parametrized, generally from experiment but in this case from ab initio calculations. The effect of the choice of the "complete" space, the model space, and the orbitals on the effective parameters will be discussed; the size of the complete space determines the degree of correlation included in the model parameters, and this permits a simple analysis of the effect of dynamical correlation on the physics of the phenomenon; we shall see that the parameters are very stable with respect to the choice of the model space but very dependent on the localized character of the orbitals. The efficiency of the derived model Hamiltonian to reproduce the "exact" spectrum is analyzed, and finally we discuss the premises of the models previously cited in light of these results. This article is restricted to the modeling of the ab initio results with few parameters and not to the analysis of the results themselves. The more physical insights of this work will be published in a separate article:[26] comparison with experiment and transferability of the effective parameters to larger systems as well as the mechanism of electron transfer.

In section 2, the way in which effective and model Hamiltonians are derived from ab initio calculations is discussed. In section 3, the methodology will be applied to the $[HCN(NH_3)_4\text{-Ru-pz-Ru}(NH_3)_4NCH]^{5+}$ molecule where pz = pyrazine, which is the well-known Creutz−Taube molecule except that two ammonia ligands have been replaced by NCH ligands to obtain a higher symmetry for the molecule. This molecule has been chosen because it is the prototype of electron transfer in mixed-valence complexes. Although we will not discuss in detail chemical insights that were obtained, we shall see that this molecule is very interesting from a methodological point of view.

2. Method

2.1. Computational Details. All calculations have been performed using the Stuttgart energy-consistent small-core RECPs (relativistic effective core potentials) and their corresponding optimized basis sets of Stuttgart. For the ruthenium atoms, the 1s−3s, 2p−3p, and 3d atomic orbitals are in the core, leaving 16 electrons explicitly described by an 8s7p6d basis contracted to 6s5p3d.[27] For the carbon and nitrogen atoms, the 1s orbital is in the core, and the 4s4p primitives are contracted to 2s2p.[28] A polarization d function (exponent = 0.8) has been added to the carbons and nitrogens of the bridging pyrazine molecule. Hydrogen atoms are described with the 3-21G basis set.[29]

Calculations have been performed using either the MOLCAS-5 program system[30] at the CASSCF (complete active space self-consistent field) and CASPT2[31] (complete active space perturbation theory at the second order) levels of theory or the DDCI2 and DDCI3 (difference dedicated configuration interaction) schemes.[32] A level shift of 0.2 has been used in the CASPT2 calculations. The DDCIn method is variational and has been implemented in the CASDI program.[33] It considers the space formed by all of the single and the following double excitations out of the CAS; if S_1 (S_3) is the space of the orbitals

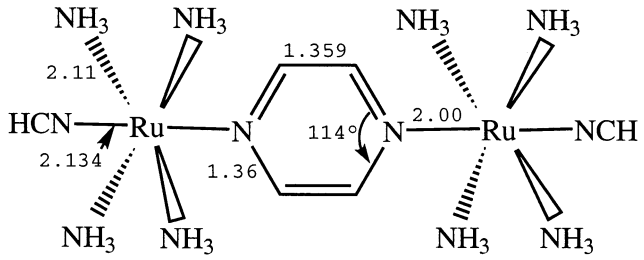

Figure 1. Scheme of the $[HCN(NH_3)_4Ru\text{-}pz\text{-}Ru(NH_3)_4NCH]^{5+}$ (pz = pyrazine) molecule with the geometrical parameters used in the calculations. Distances are in Å.

that are doubly occupied (unoccupied) in the CASCI (complete active space configuration interaction) calculation and n_h (n_p) is the number of allowed holes (particles) in S_1 (S_3), then the DDCI2 (DDCI3) space contains all of the configurations satisfying $n_h + n_p \leq 2$ (3). The option MONO is also used: it considers the space of the monoexcitations, $n_h \leq 1$ and/or $n_p \leq 1$.

Calculations are performed on the mixed-valence molecule $[HCN(NH_3)_4Ru\text{-}pz\text{-}Ru(NH_3)_4NCH\ ]^{5+}$ in the symmetrical configuration. It is a derivative of the Creutz−Taube molecule where the two axial NH_3 groups have been replaced by NCH to obtain higher symmetry. The geometry is idealized from the crystallographic data: the aromatic cycle is planar, all of the bonds around the ruthenium are perpendicular to each other, and the distances are summarized in Figure 1. The molecule belongs to the D_{2h} group. The intermetallic axis is the *x* axis, and the pyrazine ring lies in the *xy* plane.

2.2. Effective Hamiltonians. The concept of effective Hamiltonians was defined through the work of van Vleck[34] and by later works, among which those of Bloch,[35] Des Cloizeaux,[36] and Ôkubo[37] are the most important ones. The discussion will be restricted to the definition given by Bloch, which stipulates that the eigenvectors of the effective matrix are the projection of the eigenvectors of the exact matrix.

The starting point is the Schrödinger equation in the complete space, which in practice is a space as large as possible of dimension *N*.

$$\hat{H}|\Psi_m\rangle = E_m|\Psi_m\rangle \qquad m = 1, N \tag{3}$$

$|\Psi_m\rangle$ and E_m are the "exact" eigenfunctions and eigenvalues. One considers a smaller space *S*, the model space, of dimension *M* with associated projector *P*. The effective Hamiltonian $\hat{H}^{\text{eff}}$ acts only in this model space: this restriction gives the following equation:

$$\hat{H}^{\text{eff}} = P\hat{H}^{\text{eff}}P \tag{4}$$

It is such that its eigenvalues E_m are *M* of the eigenvalues of the exact Hamiltonian $\hat{H}$ and that its eigenvectors $|\tilde{\Psi}_m\rangle$ are the projections of $|\Psi_m\rangle$, the corresponding exact eigenvectors of $\hat{H}$:

$$|\tilde{\Psi}_m\rangle = P|\Psi_m\rangle \tag{5}$$

Thus, by construction

$$\hat{H}^{\text{eff}}|\tilde{\Psi}_m\rangle = E_m|\tilde{\Psi}_m\rangle \qquad m = 1, M \tag{6}$$

One defines the wave operator by

$$\Omega|\tilde{\Psi}_m\rangle = |\Psi_m\rangle \tag{7}$$

and introduces it into eq 3:

$$\hat{H}\Omega|\tilde{\Psi}_m\rangle = E_m|\Psi_m\rangle \tag{8}$$

This equation is projected onto the model space (using eq 5)

$$P\hat{H}\Omega|\tilde{\Psi}_m\rangle = E_m|\tilde{\Psi}_m\rangle \tag{9}$$

and by comparison with eq 6, one obtains the key equation

$$\hat{H}^{\text{eff}} = P\hat{H}\Omega P \tag{10}$$

Equations 6 and 9 concern only the model space, which explains why $\hat{H}\Omega$ is sandwiched by projectors *P* in eq 10. This equation can be rewritten in terms of matrices. Let us define by *C* the matrix of the coefficients of $\{|\tilde{\Psi}_m\rangle\}_{i=1,M}$ and by H^{eff} the matrix of $\hat{H}^{\text{eff}}$ in a given basis set of the model space. Equation 6 can be written

$$\hat{H}^{\text{eff}}C = SCE \tag{11}$$

where *E* is the $M \times M$ diagonal matrix containing the selected eigenvalues $\{E_i\}_{i=1,M}$ and *S* is the overlap matrix of the basis set. One easily sees that the effective Hamiltonian matrix is obtained as

$$H^{\text{eff}} = SCEC^{-1} \qquad \text{(ref 39)} \tag{12}$$

In practice, one works in an orthonormal basis set of Slater determinants: the complete space is generated by $\{\phi_i\}_{i=1,N}$, and the model space, by$\{\phi_i\}_{i=1,M}$. One calculates the *L* first roots of the Hamiltonian at a given level of the theory $\{\Psi_m = \sum_{i=1}^{N} C_{im}\phi_i\}_{m=1,L}$ $M \leq L \leq N$, with the corresponding eigenvalues E_m; these solutions are considered to be the exact ones, and a model Hamiltonian is built to reproduce them. One chooses the *M* roots of the exact Hamiltonian that have the largest weight in the model space (which maximizes $\sum_{i=1}^{M} C_{im}^2$). For simplicity, we index these roots as the first *M* ones, but they are obviously not the *M* first ones in energetic ordering. From the knowledge of these roots, one builds the $M \times M$ matrices *C* as $[C]_{im} = C_{im}$ ($i, m = 1, M$) and *E* as $[E]_{im} = E_m\delta_{im}$ ($i, m = 1, M$) and calculates the effective Hamiltonian matrix with eq 12, *S* being the unit matrix. With this procedure, one is able to build a matrix of size *M* that contains the largest conceivable amount of information concerning *M* of the roots of the exact Hamiltonian. In our case, we do not have access to the exact solutions solved as a full CI, but the complete space is as large as possible. Actually, the size of the complete space is varied to get the effective parameters at different degrees of correlation. Within this definition, the effective Hamiltonian is not Hermitian because the projection of the exact eigenvectors onto the model space is not orthogonal. In other words, matrix *C* is not unitary. Des Cloizeaux proposed a procedure to render the effective Hamiltonian Hermitian,[36] but in the molecules studied in this work and in the forthcoming article, nonhermiticity is negligeable as is shown in section 3.2: this step is thus not necessary in this work, contrary to the case studied by Calzado et al.[23]

2.3. Model Hamiltonian. The form of the model Hamiltonian is not supposed a priori. One chooses the model space, and one builds the effective Hamiltonian in this space. Then, a model Hamiltonian is proposed to reproduce as well as possible the effective Hamiltonian.

If there were no symmetry, then all of the elements of the effective Hamiltonian would be different. In this work, the molecule has high symmetry, which reduces the number of

TABLE 1: Model Hamiltonian in the Model Space Spanned by d_A, d_B, and π^*

$\lvert d_A\overline{d_A}d_B\rvert$	$\lvert d_Ad_B\overline{d_B}\rvert$	$\lvert d_A\overline{\pi^*}d_B\rvert$	$\lvert d_A\pi^*\overline{d_B}\rvert$	$\lvert\overline{d_A}\pi^*d_B\rvert$
E_0	$-t'$	t	0	$-t$
$-t'$	E_0	$-t$	t	0
t	$-t$	$E_0 + U + 2J$	$-J$	$-J$
0	t	$-J$	$E_0 + U + J$	0
$-t$	0	$-J$	0	$E_0 + U + J$

independent parameters of the effective Hamiltonian. However, some matrix elements corresponding to the same physics, for example, the transfer integral between d and π^* orbitals $t = \langle|d|\hat{h}|\pi^*\rangle$, where $\hat{h}$ is a one-electron Hamiltonian, appear as different numbers in the effective Hamiltonian because of nonhermiticity and because the core (the orbitals that are doubly occupied during the electron transfer) is not the same. However, as will be shown in the next section, the matrix elements corresponding to the same physics differ by only a few percent. Accordingly, a model parameter is calculated as the mean value of all of the effective matrix elements corresponding to the same physics. The choice of the model Hamiltonian is induced from the effective matrix: one sets equal to zero the matrix elements that are small, and one proposes a physical explanation for the other ones. Finally, one compares the eigenvalues and eigenvectors of the model Hamiltonian with the effective ones (which, let us remember, are exact as far as the ab initio results are exact) to check the validity of the modeling.

The model Hamiltonian $\hat{H}_m$ is defined by its matrix elements, as exemplified in Table 1. In this work, we use the following model parameters:

- The metal−ligand electron-transfer integral

$$t = \langle|[\text{core}]d_A||\hat{H}_m||[\text{core}]\pi^*|\rangle = \langle|[\text{core}]d_B||\hat{H}_m||[\text{core}]\pi^*|\rangle \quad (13)$$

where d_A and d_B are the d_{xz} orbitals localized on centers A and B respectively; they are the d_π orbitals overlapping with the π system of the bridging ligand. The π^* is the lowest π^* orbital of the pyrazine, and $|[\text{core}]x|$ is a Slater determinant where only orbital x is explicitly cited, the orbitals of the core being the same in the bra and the ket.

- The direct metal−metal electron-transfer integral

$$t' = \langle|[\text{core}]d_A||\hat{H}_m||[\text{core}]d_B|\rangle \quad (14)$$

- The metal−ligand exchange integral

$$J = \langle|[\text{core}]d_A\pi^*||\hat{H}_m||[\text{core}]\pi^*d_A|\rangle = \langle|[\text{core}]d_B\pi^*||\hat{H}_m||[\text{core}]\pi^*d_B|\rangle \quad (15)$$

When the d_A and the π^* orbitals are both singly occupied, then a positive value of J favors the ferromagnetic alignment of these two electrons, and a negative value favors an antiferromagnetic alignment.

- The energy gap

$$U = E(d^{11}) - E(d^{10}\pi^*) \quad (16)$$

which is the difference in energy between the manifold of configurations with one hole in a d orbital, called the d^{11} band, and the manifold of configurations with two holes in these orbitals and one electron in the lowest π^* orbital, called the $d^{10}\pi^*$ band.

3. Results and Discussion

3.1. CASSCF Results: Survey of the States. The CAS includes 15 electrons in 10 orbitals: 6 d orbitals of type t_{2g}, namely, the $d_{xz;X}$, $d_{xy;X}$, and $d_{y^2-z^2;X}$ orbitals localized on Ru_X (X = A, B), and 4 π orbitals of pyrazine—the 2 highest occupied, π_1 and π_2, and the 2 lowest unoccupied, π_1^* and π_2^*. These active orbitals are represented in Figure 2. The $d_{xz;A}$ and $d_{xz;B}$ are d_π-type orbitals overlapping with the π system of the pyrazine; they play a key role in the electron-transfer process. The $d_{xy;A}$ and the $d_{xy;B}$ are d_π-type orbitals orthogonal to this π system, whereas the $d_{y^2-z^2;A}$ and $d_{y^2-z^2;B}$ are d_δ-type orbitals. Calculations have been performed using the full symmetry of the molecule, namely, the group D_{2h}, so the d orbitals are either symmetric or antisymmetric combinations of local orbitals, but the results are much easier to interpret after a localization of the active orbitals on each metallic center. A more refined localization between the metallic center and the bridge will be discussed in section 3.2.

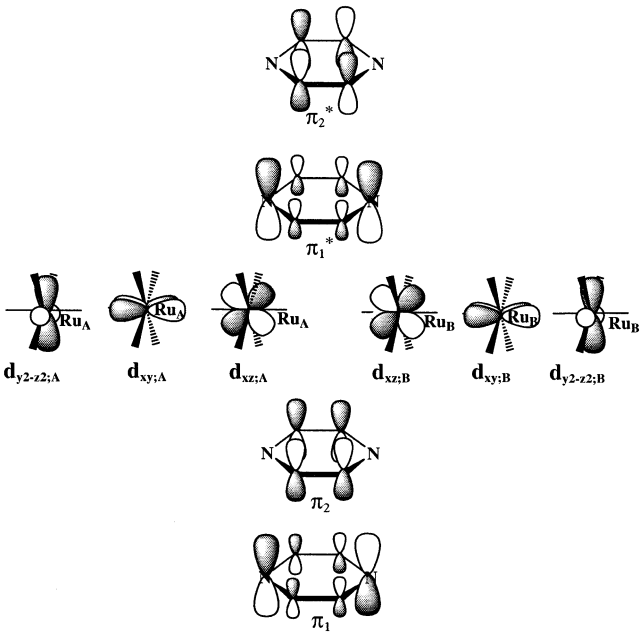

Figure 2. Schematic view of the active orbitals.

The excitation energies from the ground state up to 50 000 cm^{-1} at the state-averaged CASSCF level including eight, five, and two roots for the doublet, quartet, and sextet states, respectively, are represented in Figure 3. The spectrum can be analyzed in terms of four energy bands.

- The $d^{10}\pi_1^*$ band corresponds to all of the states in the $\pi_1^2\pi_2^2d_A^5d_B^5\pi_1^*$ configurations: there are nine such configurations, each giving rise to two doublet states and one quartet state. Six of these states are stabilized by interaction with the six states of the third band, the d^{11} band. The stabilized states are roughly a 2:1 mixture of the $d^{10}\pi_1^*$ and d^{11} bands. The ground state is one of these states; it belongs to the irrep B_{2g}, and the $d^{10}\pi_1^*$ band is restricted to configurations with holes in the $d_{xz;A}$ and $d_{xz;B}$ orbitals, whereas the d^{11} band has a hole in the gerade $^1/_2(d_A + d_B)$ orbital. The intervalence state is the lowest state of irrep B_{1u} and is composed of the same configurations as the ground state but with ungerade symmetry.

- The $d^{10}\pi_2^*$ band, lying between 25 000 and 30 000 cm^{-1}, corresponds to configurations of type $\pi_1^2\pi_2^2d_A^5d_B^5\pi_2^*$: again, there are 27 such states (9 configurations and 3 spin arrangements). This band is more compact than the previous one because the π_2^* orbital has no weight on the nitrogens, so there is only a negligeable coupling with the d orbitals.

- The d^{11} band lying between 30 000 and 35 000 cm^{-1}; this band corresponds to the states of configuration $\pi_1^2\pi_2^2d_A^{5.5}d_B^{5.5}$.

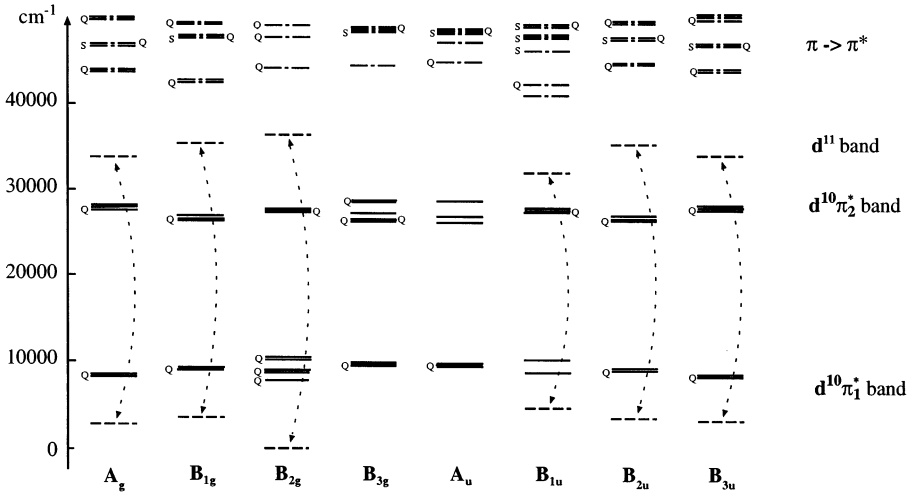

Figure 3. Energy levels in cm^{-1} of the $[HCN(NH_3)_4Ru\text{-}pz\text{-}Ru(NH_3)_4NCH]^{5+}$ molecule calculated at the CASSCF level. The reference of the energies is the ground state (B_{2g} symmetry). States are classified following their irrep, and the letter on the side denotes the spin symmetry: no letter = doublet; Q = quartet; S = sextet. The dashed arrows represent the couplings.

TABLE 2: Model Parameters *t*, *t′*, *J*, and *U* According to the Choice of Orbitals, the Model Space, and the Complete Space[a]

MOs	θ	model space	complete space	t	t'	J	U
B_{2g}	0°	$d_A\pi^*d_B$	CASCI	7285	551	−911	−22670
B_{2g}	4.64°	$d_A\pi^*d_B$	CASCI	8586	−386	0	−20888
A_{1g}	0°	$d_A\pi^*d_B$	CASCI	7937	494	−614	−21810
B_{2g}	0°	$d_A\pi^*l_B = d_{xy;B}$	CASCI	7513		−735	−21279
B_{2g}	0°	$d_A\pi^*l_B = d_{x^2-y^2;B}$	CASCI	7518		−747	−21986
B_{2g}	0°	$d_A\pi^*d_B$	MONO	6805	655	−1476	−1640
B_{2g}	4.64°	$d_A\pi^*d_B$	MONO	7016	−180	−685	−122
B_{2g}	0°	$d_A\pi^*d_B$	DDCI2	6959	600	−1517	2393
B_{2g}	4.64°	$d_A\pi^*d_B$	DDCI2	6948	−239	−721	3924
B_{2g}	0°	$d_A\pi^*d_B$	DDCI3	6954	613	−1162	−2510
B_{2g}	4.64°	$d_A\pi^*d_B$	DDCI3	7164	−238	−351	−946
B_{2g}	0°	$d_A\pi^*d_B$	MS-CASPT2	7840	395	−1035	4477
B_{2g}	4.64°	$d_A\pi^*d_B$	MS-CASPT2	7622	−481	−163	6215

[a] The orbitals are defined with respect to the irrep with which the multistate CASSCF calculations have been performed and the angle θ of mixing between the d orbitals and the π^* orbital. Energies are in cm^{-1}.

The six states belonging to this band are destabilized by the coupling with the first band; they are a 1:2 mixture of the $d^{10}\pi_1^*$ and d^{11} bands.

• Finally, the states above 40 000 cm^{-1} correspond to $\pi-\pi^*$ transitions.

As already mentioned, the physical discussion of this spectrum as well as the comparison with experiment or the dependence of the intervalence band on the bridge will be discussed in a forthcoming article.[26] However, we can already point out the astonishing fact that, in the ground state, the hole is mostly localized on the bridge and not the metal centers; it will be shown in section 3.4 that the hole is more localized on the two metalic centers once the correlation is included, and in the forthcoming article, it will be shown that it is completely localized on them for longer bridges such as bipyridine. The discussion here will be restricted to the obtaining of the model Hamiltonian, which describes only the states involving the d orbitals and the π_1^* orbital, namely, the 27 states of the $d^{10}\pi_1^*$ band and the 6 states of the d^{11} band. To shorten the notation, we will in the following sections denote the π_1^* orbital by π^* and the $d_{xz;A}$ and $d_{xz;B}$ orbitals by d_A and d_B respectively. The four other d orbitals will keep their full notation.

3.2. Effective Hamiltonian. All of the results of this section are summarized in Table 2. In each case, the effective Hamiltonian is characterized by the four parameters defined in section 2.3. As an example, the effective Hamiltonian calculated at the CASCI level is given in Table 3. The comparison with the model

TABLE 3: Effective Hamiltonian Calculated from a CASCI with Localized Orbitals of Symmetry B_{2g}[a]

$\lvert d_A\overline{d_A}d_B\rvert$	$\lvert d_Ad_B\overline{d_B}\rvert$	$\lvert d_A\overline{\pi^*}d_B\rvert$	$\lvert d_A\pi^*\overline{d_B}\rvert$	$\lvert\overline{d_A}\pi^*d_B\rvert$
30 575	−551	7331	−125	−7206
−551	30 575	−7331	7206	125
7349	−7349	6104	912	912
−97	7253	912	6972	45
−7253	97	912	45	6972

[a] Energies are in cm^{-1}.

Hamiltonian written in the same model space from Table 1 gives the value of the parameters given in Table 2. One sees that in this case there are four different values corresponding to the transfer integral t. There are different values when the transferred electron is alpha or beta, and there are two more values because of the non-Hermiticity of the effective Hamiltonian as defined by Bloch. However, the difference between the four values is very small, less than 2%, compared to other effects: t is defined as the mean value of these four numbers. The same procedure is used for the other parameters.

The first choice concerns the complete space: it is determined by the CI space and by the choice of the MOs. In a first approach, results from the CASCI are used, with the CAS comprising 15 electrons in 10 MOs as defined in section 3.1. This is the smallest CAS including valence correlation. Afterward, the complete spaces are the spaces generated by the MONO, DDCI2, and DDCI3 calculations with minimal CAS (3 electrons in 3 orbitals). Finally, the complete space is the

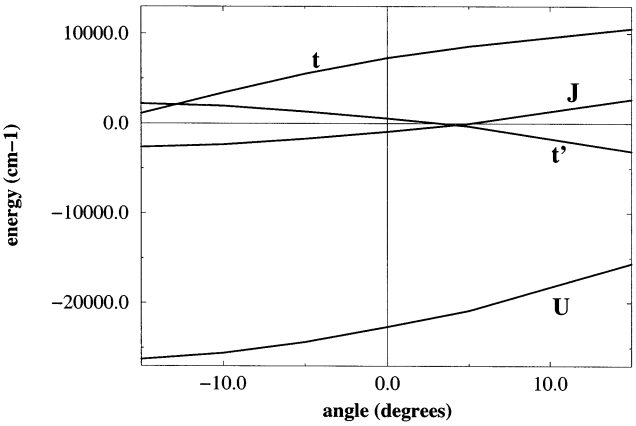

Figure 4. Dependence of the model parameters on the mixing of the active orbitals. $\theta = 0°$ corresponds to the localization following Boys' procedure.

CAS with 15 electrons in 10 orbitals, but the exact matrix is calculated at the MS-CASPT2 level of theory.

The second choice concerns the orbitals. A common set of orbitals is used for all roots and symmetries. The ungerade combination of the d_{xz} orbitals, the $1/\sqrt{2}(d_A - d_B)$ orbital, belongs to the same irrep as the π^* orbital (irrep B_{2g}), and a rotation between these orbitals affects the effective Hamiltonian matrix (eq 17). This rotation mixes the d^{11} and $d^{10}\pi^*$ bands with the $d^9\pi^{*2}$ band, and the configurations belonging to the last band are not included in the model space. In other words, the configurations of the model space spanning the effective Hamiltonian matrix do not form a complete active space; therefore, the eigenvalues of this matrix are not invariant under a rotation in the model space. But the CASCI, DDCI, or CASPT2 results are invariant under a rotation between active orbitals; thus, if the rotation is performed before the projection onto the model space, then eigenvalues of the effective Hamiltonian matrix are invariant by this operation. The three orbitals d_A, d_B, and π^* have been localized following Boys' procedure.[38] The parameters are quite sensitive to the mixing of the orbitals, as shown in Figure 4, where the model parameters are plotted with respect to θ, defined by

$$\begin{bmatrix} u' \\ \pi' \end{bmatrix} = \begin{bmatrix} \cos\theta & -\sin\theta \\ \sin\theta & \cos\theta \end{bmatrix} \begin{bmatrix} (d_A - d_B)/\sqrt{2} \\ \pi^* \end{bmatrix} \qquad (17)$$

A rotation of 1° affects t and U by about 400 cm^{-1} and J and t' by about 200 cm^{-1}. $\theta = 0°$ corresponds to the angle obtained by Boys' procedure. Canonical orbitals are obtained at $\theta = 10°$. t' and J become zero for $\theta = 2.83$ and 4.64°, respectively, which are quite small angles. The localization of the orbitals almost corresponds to the annihilation of the exchange integral J and the direct metal−metal transfer integral t'. We point out again that all of the sets of parameters of Figure 4 give the same eigenvalues and thus have the same ability to model the system. In the following discussion, results for both $\theta = 0$ and 4.64° will be discussed, namely, the mixing obtained through Boys' localization procedure and the one corresponding to the annihilation of the zeroth-order contribution to the exchange integral, that is, J at the CASSCF level.[40] It has to be mentioned that large mixing (above ±10°) gives rise to a large non-Hermiticity of the effective Hamiltonian due to the neglect of the $d^9\pi^{*2}$ configuration in the model space.

We have also compared the influence of the symmetry of the orbitals: two sets of MOs optimized at the CASSCF level averaged over eight roots either in $^2B_{2g}$ symmetry, the symmetry of the ground state, or $^2A_{1g}$ symmetry have been compared. The results are similar; the discrepancy seems to be due more to the localization procedure than to the discrepancy in the eigenvalues. In the following discussion, MOs of $^2B_{2g}$ symmetry are used.

The third choice is the model space; it is defined by Slater determinants of localized orbitals. The first one is spanned by the three orbitals d_A, d_B, and π^* limited to configurations d^{11} and $d^{10}\pi^*$ as in Tables 1 and 3; this model space gives model interactions between the d_{xz} and π^* orbitals. To determine interaction involving the other d orbitals and to check the generality of the model Hamiltonian, we have tried other model spaces spanned by the determinants $|d_A\overline{d_A}l_B|$, $|d_A\pi^*\overline{l_B}|$, $|d_A\overline{\pi^*}l_B|$, and $|\overline{d_A}\pi^*l_B|$ where l_B is either $d_{x^2-y^2;B}$ or $d_{xy;B}$. The effective Hamiltonian calculated in these model spaces can be modeled only by the parameters described in section 2.3; as expected, the interaction between the $d_{y^2-z^2}$ or d_{xy} orbitals and the π^* orbital is very small. A comparison of the values of the model parameters calculated with different model spaces (Table 2) shows that the discrepancy is hundreds of cm^{-1}, except for U, which is understable because different configurations are considered; a hole in a d_{xz} orbital is not equivalent to a hole in a $d_{y^2-z^2}$ or a d_{xy} orbital. This shows that model parameters calculated with a model space can be used to describe states not belonging to this model space; in other words, although the form of the model Hamiltonian is induced by the effective Hamiltonian in a given model space, this model Hamiltonian does not depend of the choice of the model space as long as the model space includes the same active orbitals. This point is crucial to the validity of the procedure. If the model space includes more orbitals, then it will be necessary to add more parameters to the model Hamiltonian.

In conclusion to this section, the effective Hamiltonian method described in section 2.2 applied to the $[HCN(NH_3)_4$-Ru-pz-$Ru(NH_3)_4NCH]^{5+}$ molecule leads to matrices that are almost Hermitian and that are easily reproduced by a simple model Hamiltonian. This model Hamiltonian does not depend on the choice of model space as long as it involves the same active orbitals, but it is strongly affected by the localization of the d and π^* orbitals.

3.3. Model Hamiltonian. The previous section suggests that the modeling of the $[HCN(NH_3)_4Ru$-pz-$Ru(NH_3)_4NCH]^{5+}$ molecule by a two-parameter Hubbard-like Hamiltonian is the most reasonable one: t is the one-electron coupling between the d_{xz} and π^* orbitals, and U is the difference in energy between the d^{11} and $d^{10}\pi^*$ bands, independent of which d orbitals the hole(s) is (are) located. t' and J are quite small and depend too much on the mixing of the orbitals to have real significance. It is noteworthy that t' and J vanish almost at the same degree of mixing between orbitals $^1/_2(d_A - d_B)$ and π^*, an angle close to Boys' localization angle. These two parameters are different in nature, the first one being a one-electron and nonlocal term that should vanish when there is destructive interference in the interaction between the tails of the d_A and d_B orbitals whereas J is a two-electron and more local term because it describes the interaction between nearest neighbors. The choice of a two-parameter model is nonambiguous because there is only one set of parameters reproducing the energies, contrary to the four-parameter model in which there are an infinite number of parameter sets giving the same energies. With the two parameters t and U, one can describe the 33 states involving the d^{11} and $d^{10}\pi^*$ bands because the difference in energy between the configurations with holes in different types of d orbitals is not important. Surprisingly, U is negative at the CASSCF level,

the $d^{10}\pi^*$ band lies below the d^{11} band, and the contribution of the d^{11} band to the ground state is about $^1/_3$. The ability of the model Hamiltonian to reproduce the exact spectrum is characterized by the standard deviation defined as

$$\mathrm{std} = \sqrt{\frac{1}{N}\sum_{i=1}^{N}(\Delta_i - \bar{\Delta})^2} \qquad (18)$$

N is the number of transitions, $\Delta_i = E_i^{\mathrm{mod}} - E_i^{\mathrm{abin}}$ is the difference between the energy of the ith transition modeled by the model Hamiltonian and calculated by the ab initio method, and $\bar{\Delta}$ is the mean value of Δ_i. The standard deviation is on the order of 1000 cm^{-1} at the CASSCF level, which means that the main effects are taken into account and the accuracy is quite good for a two-parameter model describing 33 states spanning 35 000 cm^{-1}.

The usual way to extract model parameters is to calculate the parameters of the model Hamiltonian by least-squares fitting from the ab initio energies. In this case, by fitting the four transitions generated by the model space given in Table 1 calculated at the CASCI level with two parameters U and t, one obtains $U = -20\,761$ cm^{-1} and $t = 8684$ cm^{-1} with a standard deviation of 900 cm^{-1} in the description of the 33 states. These values are very close to the ones obtained by the effective Hamiltonian method. A least-squares fitting with four parameters is not really a fit because there are as many variables as equations. The solutions of this nonlinear system are four sets of solutions $\{U, t, J, t'\}$: {18955, ±9550, 912, −1227} and {23235, ±6736, −1227, 912} (all numbers are in cm^{-1}). These sets of parameters correspond to within 10 cm^{-1} to the results obtained with the effective Hamiltonian technique with θ equal to 9 and −1.7° respectively. The results of the least-squares fittings compared to the effective Hamiltonian approach show that both methods give almost the same results. For the two-parameter model, there is no ambiguity, so the obtained parameters are the same. For the four-parameter model, the least-squares procedure gives four solutions out of an infinite number of solutions. In conclusion, the two methods give consistent results; the least-squares fitting procedure is easier to apply but provides perhaps less insight.

3.4. Introduction of Dynamical Correlation. All of the results of this section are summarized in Table 2. The size of the complete space has been increased to introduce the effect of the dynamical correlation. Calculations have been performed at the MONO, DDCI2, and DDCI3 levels using a restricted CAS of three electrons in three orbitals—d_A, d_B, and π^*—and MS-CASPT2 with the CAS with 15 electrons in 10 MOs as described before. The dynamical correlation is larger in the d^{11} band than in the $d^{10}\pi^*$ band because there is one more doubly occupied orbital in the first one, which is furthermore rather atomic. Thus, contracted methods (i.e., methods in which the coefficients of the zeroth-order wave function are kept fixed) such as SS-CASPT2 (single state CASPT2) are not suitable for this molecule. Results are obtained with the set of localized orbitals of symmetry B_{2g} for $\theta = 0$ and 4.64° as in section 3.2; CASPT2 calculations were performed after a CASCI calculation performed on a common set of orbitals, which are the same orbitals that were used for the DDCI calculations.

The first conclusion is that the form of the effective Hamiltonian matrix is not affected by correlation; the matrix remains quasi-Hermitian, coefficients that are negligible at the CASCI level remain negligible, and matrix elements corresponding to the same physical parameters are almost identical. The main effect of correlation is a reduction of the energy gap between the two previously mentioned bands: it becomes almost zero at the correlated level. There are oscillations: still negative at the MONO level, they becomes positive at the DDCI2 level, again negative at the DDCI3 level, and finally positive at the CASPT2 level. The respective weights of the ground state on the d^{11} and $d^{10}\pi^*$ bands are 0.30/0.45 for DDCI3 and 0.67/0.27 for CASPT2. In the limit of full CI, the two configurations must be almost degenerate, and the ground state must have almost equal weights of these two bands. The introduction of dynamical correlation has little effect on the transfer integrals t and t'; t is very stable from the CASCI to the DDCI3 calculation and 1000 cm^{-1} larger at the CASPT2 level, but the discrepancy is reasonable given the total difference in the methods. The effect of correlation is larger on the exchange integral J. At the CASSCF level, $\theta = 4.65°$ corresponds to the annihilation of the zeroth-order ferromagnetic contribution, the so-called potential exchange by Anderson.[40] The monoexcitations (MONO) introduce an antiferromagnetic contribution ($J = -685$ cm^{-1}) that is partially compensated for by the introduction of the double excitations of the DDCI3 space ($J = -351$ cm^{-1}). J calculated by the CASPT2 method is slightly smaller ($J = -163$ cm^{-1}).

The introduction of correlation does not influence the qualitative conclusions of the last section. The description of this molecule by means of a few model parameters permits a straightforward analysis of the effect of correlation, and it is noteworthy that variational method such as DDCI3 and a perturbative method such as MS-CASPT2 give similar results.

4. Conclusions

In this article, the effective Hamiltonian technique has been used to propose a model Hamiltonian for a bridged mixed-valence molecule. It is inspired by the work of Malrieu and co-workers,[23] who used this technique on magnetic systems. All calculations have been performed on a benchmark molecule, which is a mixed-valence dimer of ruthenium that is closely related to the Creutz−Taube molecule, the $[HCN(NH_3)_4Ru\text{-}pz\text{-}Ru(NH_3)_4NCH]^{5+}$ molecule, where pz = pyrazine. We have analyzed the vertical spectrum of this molecule and have shown that two bands of configurations play a crucial role in the lowest part of the spectrum: the d^{11} and $d^{10}\pi^*$ bands with respectively one and two holes in the d orbitals. An ab initio calculation is first performed, and results are projected using Bloch's effective Hamiltonian technique in a model space spanned by a d orbital localized on Ru_A, the lowest π^* orbital of the pyrazine, and another d orbital localized on Ru_B. This effective matrix is modeled by parameters whose physical meaning is easy to analyze. Thirty-three states of this spectrum can be well reproduced with two parameters: U, the energy gap between the two previous bands, and t, the transfer integral between the d_π orbitals that overlap with the π system of the pyrazine and the lowest π^* orbital of the pyrazine. This model can be refined by the introduction of two more parameters: the exchange integral J between the two mentioned orbitals and the direct transfer integral t' between the two metallic centers. Contrary to what is expected, the $d^{10}\pi^*$ band is the most stable one at the CASSCF level, and the ground state has a weight of about $^2/_3$ from this configuration. Dynamical correlation is introduced by means of variational methods such as DDCI or perturbative methods such as MS-CASPT2; the same form of the model Hamiltonian is found, and the main effect of correlation is the reduction of the energy gap U, which becomes almost zero.

The advantage of this method in calculating model parameters is that there is not any a priori assumptions of the form of the

model Hamiltonian, and we have demonstrated that we obtain the same model Hamiltonian with several different choices of model spaces. For example, for the studied molecule, one expected a model with two parameters: t and U. To refine it, one would add one parameter, t', without necessarily including J. Furthermore, we have shown the crucial effect of the localization of the orbitals: a very small amount of mixing between the orbitals has a considerable effect on the effective parameters, whereas it has no effect on the eigenvalues of the system. This must not be seen as a drawback of this technique but as a weak point of model Hamiltonians. They are based on the idea of local orbitals, which is a very practical mental representation of the molecule but is ambiguous in practice. We show that there is an angle of mixing close to the one obtained with Boys' procedure where J and t' are almost zero. For other angles, the variation in U and t is compensated for by variations of J and t'. The conclusion is that the lower vertical excitation spectrum of the $[HCN(NH_3)_4Ru\text{-}pz\text{-}Ru(NH_3)_4NCH]^{5+}$ molecule can be modeled by a two-parameter model Hamiltonian expressed in the set of localized orbitals where t' and J vanish.

Finally, the results were compared with the more traditional method, where model parameters are extracted by least-squares fitting. The results were consistent, but the method proposed by this article provides more physical insight, especially concerning the chemical analysis of the mixing of the orbitals and of secondary effects. This method has been applied to molecules with longer bridges and has permitted a check of the transferability of the model parameters and an extraction of parameters describing internal transfer in the bridge. These results will be published in a forthcoming article.[26]

The models proposed in the 1980s were based on the idea that the molecule could be divided into units—two terminal units on the two metallic centers and intermediate units on the bridging ligand. Furthermore, all of the developments supposed that the transfer integral t is small compared to the excitation energy U. What results from this work is that a two-parameter model is completely valid for the description of such systems but that in this special molecule the assumption that $|t/U| \ll 1$ that was used to develop the perturbative estimation of eq 1 is not valid. However, this molecule is really a pathological case for this approximation because U is almost zero, the hole hopping without energy cost between the metallic centers and the bridge. Furthermore, the two-band Hubbard Hamiltonian of eq 2 is completely justified by this work and even in a more generalized form, namely, including all of the occupied d orbitals of ruthenium.

The parameters that we have obtained compare well to parameters that were fit from experiment:[19−21] our value of t is slightly larger than the values proposed in the Introduction by 1000−2000 cm^{-1}, which is a reasonable discrepancy. The value of U for the monomer will be discussed in the forthcoming article, and the value of U for the binuclear molecule of 3500 cm^{-1} is compatible with this work, where we have shown that this parameter is very sensible for the degree of correlation included in the ab initio calculation; at least the experimental value falls between the DDCI3 and CASPT2 values.

A key result is that the fundamentals of a simple modeling of a bridged mixed-valence compound in the tight-binding approximation with a transfer integral between nearest neighbors and an energy gap are validated by this work.

Acknowledgment. I thank Jean-Paul Malrieu for having taught me the effective Hamiltonian technique. The starting point of this article is unpublished work done by Jean-Paul Malrieu and me in 1998 on a model system. I thank Trond Saue for critically reading the manuscript. Calculations have been carried out either at the IDRIS (Orsay, France) through a grant of computer time from the Conseil Scientifique or at the CURRI (Strasbourg, France).

References and Notes

(1) Creutz, C.; Taube, H. J. *J. Am. Chem. Soc.* **1969**, *91*, 3988.
(2) *Electron Transfer in Chemistry*; Balzani, V., Ed.; Wiley-VCH: Weinheim, Germany, 2001.
(3) Brunschwig, B. S.; Sutin, N. *Coord. Chem. Rev.* **1999**, *187*, 233.
(4) Launay, J.-P. *Chem. Soc. Rev.* **2001**, *30*, 386.
(5) Newton, M. D. *Chem. Rev.* **1991**, *91*, 767.
(6) Larsson, S. J. *J. Am. Chem. Soc.* **1981**, *103*, 4034.
(7) Beratan, D. N.; Hopfield, J. J. *J. Am. Chem. Soc.* **1984**, *106*, 1584.
(8) Ratner, M. A. *J. Phys. Chem.* **1990**, *94*, 4877.
(9) Joachim, C. *Chem. Phys.* **1987**, *116*, 339.
(10) McConnell, H. M. *J. Chem. Phys.* **1961**, *35*, 508.
(11) Davis, W. B.; Ratner, M. A.; Wasielewski, M. R. *Chem. Phys.* **2002**, *281*, 333.
(12) Petrov, E. G.; Zelinskyy, Y. R.; May, V. *J. Phys. Chem. B* **2002**, *106*, 3092.
(13) Napper, A. M.; Read, I.; Kaplan, R.; Zimmt, M. B.; Waldeck, D. H. *J. Phys. Chem. A* **2002**, *106*, 5288.
(14) Villani, G. J. *J. Chem. Phys.* **2002**, *117*, 1279.
(15) Hubbard, J. *Proc. R. Soc. London* **1964**, *285*, 542.
(16) Ondrechen, M. J.; Gozashti, S.; Wu, X. M. *J. Chem. Phys.* **1992**, *96*, 3255.
(17) Ferretti, A.; Lami, A. *Chem. Phys.* **1994**, *181*, 107.
(18) Ferretti, A.; Lami, A.; Murga, L. F.; Shehadi, I. A.; Ondrechen, M. J.; Villani, G. *J. Am. Chem. Soc.* **1999**, *121*, 2594.
(19) Zwickel, A. M.; Creutz, C. *Inorg. Chem.* **1971**, *10*, 2395.
(20) Creutz, C.; Newton, M. D.; Sutin, N. *J. Photochem. Photobiol., A* **1994**, *82*, 47.
(21) Ferretti, A.; Lami, A.; Villani, G. *Inorg. Chem.* **1998**, *37*, 2799.
(22) Durand, P.; Malrieu, J.-P. In *Ab Initio Methods in Quantum Chemistry*; Lawley, K. P., Ed.; Wiley & Sons: Chichester, U.K., 1987.
(23) Calzado, C. J.; Cabrero, J.; Malrieu, J.-P.; Caballol, R. *J. Chem. Phys.* **2002**, *116*, 3985.
(24) Joachim, C.; Launay, J. P. *Chem. Phys.* **1986**, *109*, 93.
(25) Sanz, J. F.; Malrieu, J.-P. *J. Phys. Chem.* **1993**, *97*, 99.
(26) Bolvin, H. To be submitted for publication.
(27) Andrae, D.; Haeussermann, U.; Dolg, M.; Stoll, H.; Preuss, H. *Theor. Chim. Acta* **1990**, *77*, 123.
(28) Bergner, A.; Dolg, M.; Kuechle, W.; Stoll, H.; Preuss, H. *Mol. Phys.* **1993**, *80*, 1431.
(29) Binkley, J. S.; Pople, J. A.; Hehre, W. J. *J. Am. Chem. Soc.* **1980**, *102*, 939.
(30) Andersson, K.; Barysz, M.; Bernhardsson, A.; Blomberg, M. R. A.; Carissan, Y.; Cooper, D. L.; Cossi, M.; Fleig, T.; Fülscher, M. P.; Gagliardi, L.; de Graf, C.; Hess, B. A.; Karlström, G.; Lindh, R.; Malmqvist, P.-Å.; Neogrády, P.; Olsen, J.; Roos, B. O.; Schimmelpfennig, B.; Schütz, M.; Seijo, L.; Serrano-Andrés, L.; Siegbahn, P. E. M.; Stålring, J.; Thorsteinsson, T.; Veryazov, V.; Wierzbowska, M.; Widmark, P.-O. *MOLCAS*, version 5.2; Lund University: Sweden, 2001.
(31) Andersson, K.; Malmqvist, P.-Å.; Roos, B. O.; Sadlej, A. J.; Wolinski, K. *J. Phys. Chem.* **1990**, *94*, 5483.
(32) Miralles, J.; Daudey, J.-P.; Caballol, R. *Chem. Phys. Lett.* **1992**, *198*, 555.
(33) Benamor, N.; Maynau, D. *Chem. Phys. Lett.* **1998**, *286*, 211.
(34) Van Vleck, J. H. *Phys. Rev.* **1929**, *33*, 467.
(35) Bloch, C. *Nucl. Phys.* **1958**, *6*, 329.
(36) Des Cloizeaux, J. *Nucl. Phys.* **1960**, *20*, 321.
(37) Ôkubo, S. *Prog. Theor. Phys.* **1954**, *12*, 603.
(38) Boys, S. F. *Rev. Mod. Phys.* **1960**, *32*, 296. Forste, J. M.; Boys, S. F. *Rev. Mod. Phys.* **1960**, *32*, 300. Program provided by Nicolas Suaud.
(39) This equation is equivalent to eq 9 of ref 24, which in our notation becomes $\langle\phi_i|\hat{H}^{\text{eff}}|\phi_j\rangle = \sum_{n,p=1}^{M}[C^{-1*}]_{ni}[C^{-1}]_{pj}E_p\langle\Psi_n|\tilde{\Psi}_p\rangle = \sum_{n,p,l,k=1}^{M}[C^{-1*}]_{ni}[C^{-1}]_{pj}E_pC^*_{kn}S_{kl}C_{lp} = \sum_{p,l=1}^{M}S_{il}C_{lp}E_p[C^{-1}]_{pj}$, which is exactly the same as eq 12. One uses the fact that $\sum_{n=1}^{M}C_{kn}*[C^{-1*}]_{ni} = \delta_{ki}$ to simplify the previous identity.
(40) Anderson, P. W. In *Magnetism*; Rado, G. T., Suhl, S., Eds.; Academic Press: New York, 1963; Vol. 1, p 25.